Ocean Dynamics (2011) 61:717–730
DOI 10.1007/s10236-011-0404-9

The influence of meteorological variation on the upwelling system off eastern Hainan during summer 2007–2008

Jian Su · Jun Wang · Thomas Pohlmann · Dongfeng Xu

Received: 4 March 2010 / Accepted: 8 March 2011 / Published online: 16 April 2011

Abstract The influence of meteorological variation, i.e., typhoon and precipitation events, on the coastal upwelling off the eastern Hainan Island was studied based on observations taken during two upwelling seasons. The observations were made in August 2007 and July 2008, respectively. We found that, in principle, similar structure of sea surface temperature and bottom temperature prevailed in both observational periods, providing evidence that upwelling events occur frequently during the summer monsoon along the eastern Hainan shelf. Based on a simple momentum balance theory, we studied the balances between momentum fluxes, wind stress, and bottom stress. The results showed that the Burger number is $S \approx 1$, indicating that the cross-shelf momentum flux divergence was balanced by the wind stress and the onshore return flow occurred in the interior of the water column. Hence, a conceptual model of the upwelling structure was built for further understanding of upwelling events. In addition, it was also observed that variations in the strength of upwelling are controlled by storm events, i.e., strong northerly winds change the structure of the thermocline on the shelf significantly. The strong mixing caused by wind reduces the strength of the thermocline, in particular in coastal seas. Based on our conceptual model, a frontal zone between mixed coastal water and offshore water develops which destabilizing the water column and hence decreases the upwelling strength. Freshwaters from the two main rivers in the Wenchang Bay are confined to the coastal area less than 20–30 m deep, as confirmed by our water mass analysis. Freshwater discharge stabilized the water column, inhibiting the upwelling as shown by the potential energy calculation. Consequently, estuarine water only inhibits the upwelling in the near coastal area. Therefore, it can be concluded that estuarine water does not have a significant impact on upwelling strength on the shelf.

Keywords Hainan · Upwelling dynamics · Observational data · Thermocline

Responsible Editor: John Wilkin

J. Su (✉) · T. Pohlmann
Institute of Oceanography, Centre for Marine and Climate Research, University of Hamburg, Bundesstr. 53, 20146 Hamburg, Germany
e-mail: Jian.Su@zmaw.de

J. Su
Institute for Coastal Research, GKSS Research Center, Max-Planck-Str. 1, 21502 Geesthacht, Germany

J. Wang · D. F. Xu
State Key Laboratory of Satellite Ocean Environment Dynamics, Second Institute of Oceanography, State Oceanic Administration, Hangzhou 310012, China

1 Introduction

Continental shelves exhibiting wind-driven coastal upwelling have been studied for decades because of high biologically productivity in these areas (Pedlosky 1978; Lentz 1992; Smith 1995; Allen et al. 1995; Federiuk and Allen 1995; Gan and Allen 2002). There exists a strong upwelling along the northern South China Sea (SCS) shelf break, which has a strong influence on shelf circulation (Jing et al. 2009). Guo et al. (1998) estimated the location and magnitude of the maximum vertical velocity using both a diagnostic model and observations

at eastern Hainan shelf. However, the water volume transported to the shelf induced by upwelling events has not been estimated. Recently, there have been some studies on upwelling around Hainan Island (Lü et al. 2008; Su and Pohlmann 2009). Nevertheless, the dynamics of the upwelling, such as upwelling structure, the influence of wind events, and response of estuarine water, is not yet fully understood.

There have been relatively few hydrographic surveys on the northern SCS shelf (Su 2004). In summer, upwelling and cold eddies, both associated with increased nutrient levels and high primary production, have been confirmed only by the modeling studies of Ning et al. (2004). Therefore, it seems appropriate to analyze the shelf response to upwelling by combining our observational data with information from other available datasets. Indeed, the most important effect of upwelling is its capability of bringing nutrient-rich waters from the deep ocean to the shelf and estuaries. Hence, we aim to understand the dynamical changes in shelf circulation due to upwelling. In this context, a conceptual model of upwelling induced circulation has been developed and to provide an estimate of the flux from offshore to the shelf area.

The eastern Hainan shelf is relatively narrow, which has an influence of the permanent stratification in this area. When a wind-driven upwelling is acting on a stratified ocean, the development of a jet depends on the strength of the stratification, and the coastal upwelling is confined to an area 30 km off the coast (O'Brien and Hurlburt 1972; Allen 1973). The interaction between wind-driven upwelling and stratification could also occur on different spatial scales. Monteiro and Largier (1999) found that, in the southern Benguela system, wind drives upwelling raises bottom water, which strengthens stratification on a regional scale; conversely, on the local bay scale, wind drives vertical mixing which weakens stratification. Therefore, the knowledge of the dynamics of the upwelling system off eastern Hainan could also help to understand other similar upwelling systems.

On the eastern Hainan shelf, we can find two estuaries and several lagoons enclosed by coral reefs, which has a typical tropical geographical characteristics. The study of the estuaries response to upwelling may provide a reference base for similar type along the tropical coasts (Ye 1988). Thus, we aim at three major topics in this study: (1) the balance between momentum flux divergence, wind stress, and bottom stress based on existing theory; (2) the impacts of storms on the strength of upwelling; and (3) the influence of estuaries, including coastal zone, on upwelling.

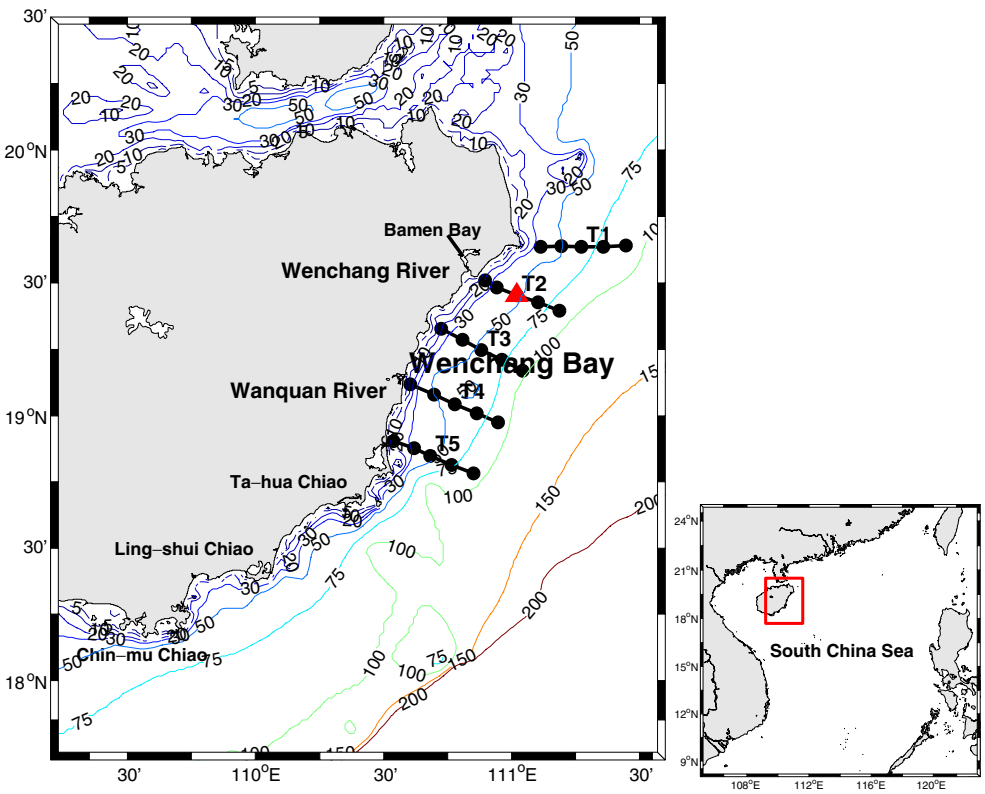

Fig. 1 Topography (meters) of the eastern Hainan shelf with sampling sites covered during the cruises August 2007 and July 2008 and five sections T1–T5 from north to south are defined. The *black dots* are sampling stations. The *red triangle* is the anchor station for current measurements. There exist two major rivers in the Wenchang Bay, i.e., Wanquan River and Wenchang River. The *red square in the right panel* shows the location of eastern Hainan Island in the South China Sea

2 Data and methods

2.1 Cruise data

To detect the spatial and temporal variability in the eastern Hainan upwelling area, two cruises were conducted from 19 to 22 August 2007 and from 27 to 31 July 2008 on the eastern Hainan shelf (Fig. 1). Conductivity, temperature, and depth (CTD) data, current meter data, and chemical parameters were obtained, and temperature and salinity data were measured with a SeaBird SB19 CTD system at each station. Five sections have been selected which run perpendicular to the coastline, covering the area of upwelling influence. It has to be noted that salinity during the cruise in 2007 was measured from water samples because of a calibration problem with the salinity measured by our CTD instrument. A 16-h anchor station was conducted in the center of section T2 during the cruise in 2007. A current meter was used to measure velocities at 5, 25, and 50 m depth, separately. From these data, we calculated the mean currents to perform a qualitative cross-shelf momentum flux study. During the July 2008 cruise, several stations near the Wenchang River and Wanquan River estuaries were sampled (river locations are shown in Fig. 1). These near coastal stations were used to analyze the impact of upwelling on the estuaries.

It is noted that the weather was different in both observational periods. In August 2007, the observations took place following a typhoon event (10 August; Fig. 2; typhoons tracks can be found at http://www.solar.ifa.hawaii.edu/Tropical/GifArchive/PABUK-07.gif). Interestingly, a typhoon event (8 August) affected our observational area right after the observations in July 2008, which obviously had no impact on our measurement. The typhoon in 2007 was associated with strong northerly winds, which had a large influence on

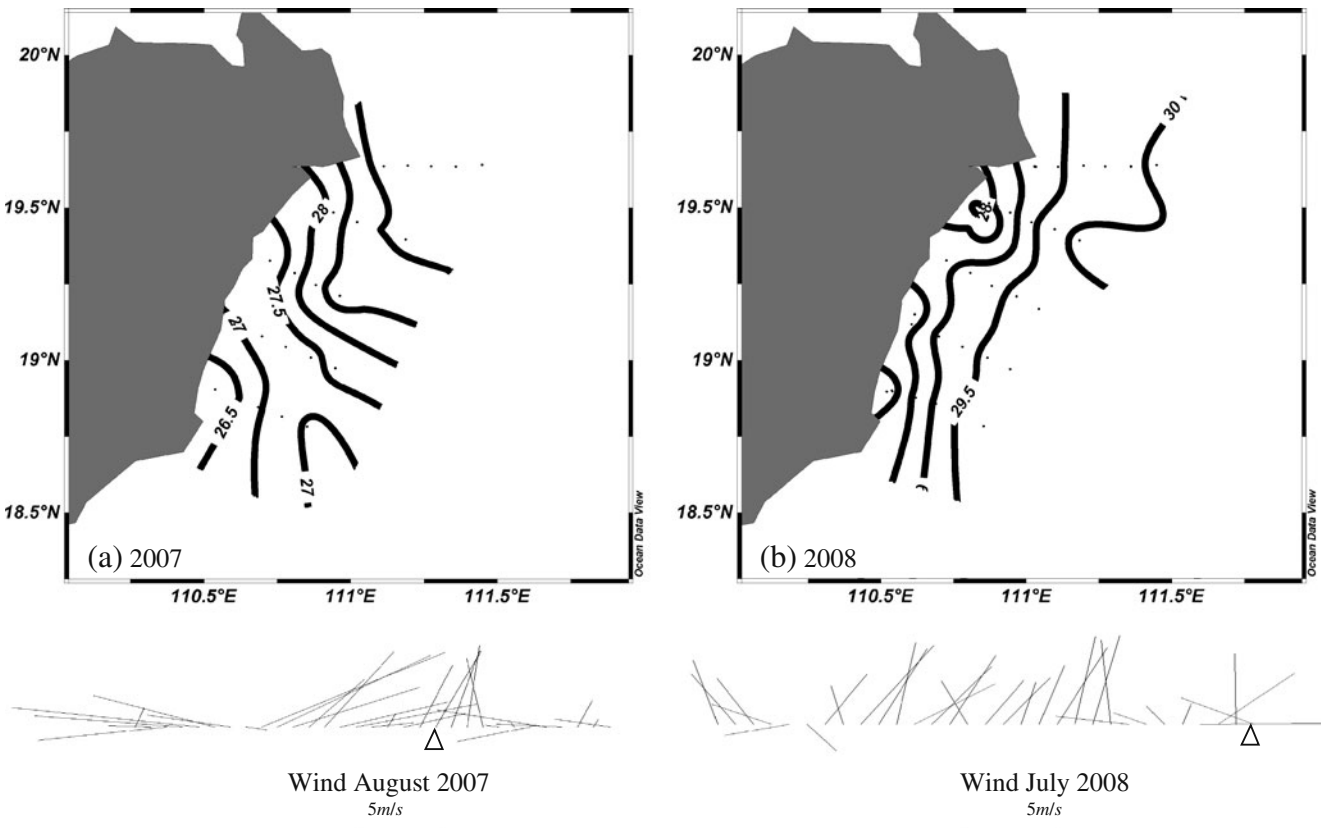

Fig. 2 Observed SST distribution during the cruises 19–22 August 2007 (**a**) and 27–31 July 2008 (**b**). They showed similar cold water center which exists at southwestern corner of the bay. The *vector plots* are daily averaged wind velocities representative for the observational area during the month in which the observation was carried out, and the *triangles* at the *x*-axis give the observed period. It is obvious that the measurement campaign took place after a typhoon event in August 2007, which could be defined as post-storm upwelling stage. Conversely, the observations in August 2007 carried out before a wind event, which could be defined as a pre-storm stage

the coastal environment. During the summer monsoon, typhoons always generate a large disturbance of the coastal ecosystem on the northern South China Sea shelf. With respect to the occurrence of typhoon winds, we define the upwelling in 2007 as post-storm stage and in 2008 as pre-storm stage. Notably, these strong winds are not favorable for upwelling in general, since normally strong northerly wind outbreaks are related to typhoons, which theoretically should induce an Ekman downwelling.

2.2 Relevant data

Sea surface temperature (SST) data are provided by the Operational SST and Sea Ice Analysis (OSTIA) system. OSTIA uses satellite SST data, provided by international agencies via the Global Ocean Data Assimilation Experiment High-Resolution SST Pilot Project regional/global task sharing framework, which is available online (http://ghrsst-pp.metoffice.com/pages/latest_analysis/ostia.html).

The sea surface height (SSH) data presented in this paper are based on the new products of the Modular Ocean Data Analysis System (MODAS; Kara and Barron 2007). The MODAS SSH products are used to obtain a synoptic overview of the reaction of SSH during two observational periods in 2007 and 2008 during upwelling events (Fig. 3).

The latest of the wind-measuring satellites, NASA's Quick Scatterometer (QuikSCAT), was launched into orbit on 19 June 1999. The data are available online at http://podaac.jpl.nasa.gov/quikscat. We use its daily averaged wind vector close to the observational area to detect the wind situation during the months of 2007 and 2008 when our campaigns were conducted.

The precipitation data in stations of Haikou and Qionghai were used to obtain the information of river discharge difference in both years. The precipitation in Haikou is related to river discharge from the Wenchang River, while that in Qionghai represents the river discharge from the Wanquan River. The data are available online (Climate Center, Utah State University; http://climate.usurf.usu.edu/products/data.php?tab=gsod).

3 Results

3.1 Thermocline variation at different wind stages

The observed SST in both years showed a similar structure, i.e., the onshore site of the southern section T5 is the coldest (Fig. 2), due to topographic influence. This is confirmed by the model studies of Su and Pohlmann (2009). Looking at the Wenchang and Wanquan estuaries in 2008 (Fig. 2b), there is obviously an influence of river discharge bringing cold water to the shelf sea. These two rivers originate in the nearby high mountain range in the center of the island. As a result, the water is relatively cold compared to coastal waters. We conducted one station near the Wanquan

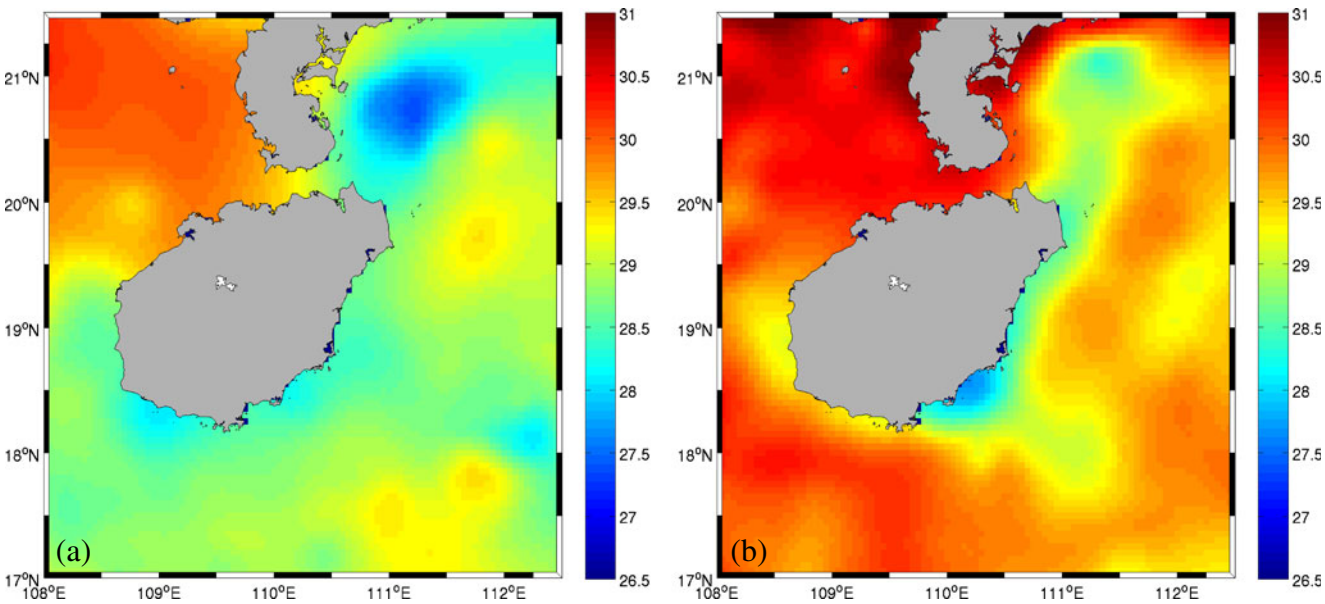

Fig. 3 Satellite measured SST (°C) on 20 August 2007 (**a**) and on 28 July 2008 (**b**). The temperature is significantly lower in 2007 which is caused by influence of typhoon

River mouth during the cruise in 2008 having a surface temperature of 26°C supporting this hypothesis. The bottom temperature indicates a warm water center near the Wenchang estuary (Fig. 4a, b). The structure of a surface cold water center and a bottom warm water center show a strong coherency with topographic features in this bay. As discussed above, the weather during these two investigation periods was considerably different, e.g., the cruise in August 2007 took place after a typhoon event (Fig. 2, wind plots). The consistency of the hydrographic structure in different years under different weather conditions confirms that the hydrodynamical conditions in the observational area are strongly influenced by topographic effects.

However, there are still visible differences between these two observational records. Temperatures in 2007 were colder than that in 2008, from which we could speculate that the typhoon brought cold water from the northern SCS shelf to the observational area. Besides the difference in SST, the salinity in the Wanquan estuary (section T4) is much lower in 2007, which definitely relates to the typhoon event (Fig. 4c). According to the wind strength and direction during the month of observation, we can define the upwelling event in August 2007 as post-storm stage and that in July 2008 as a pre-storm stage. According to this obvious difference in meteorological forcing, we can speculate that a stronger mixing after the strong wind event or

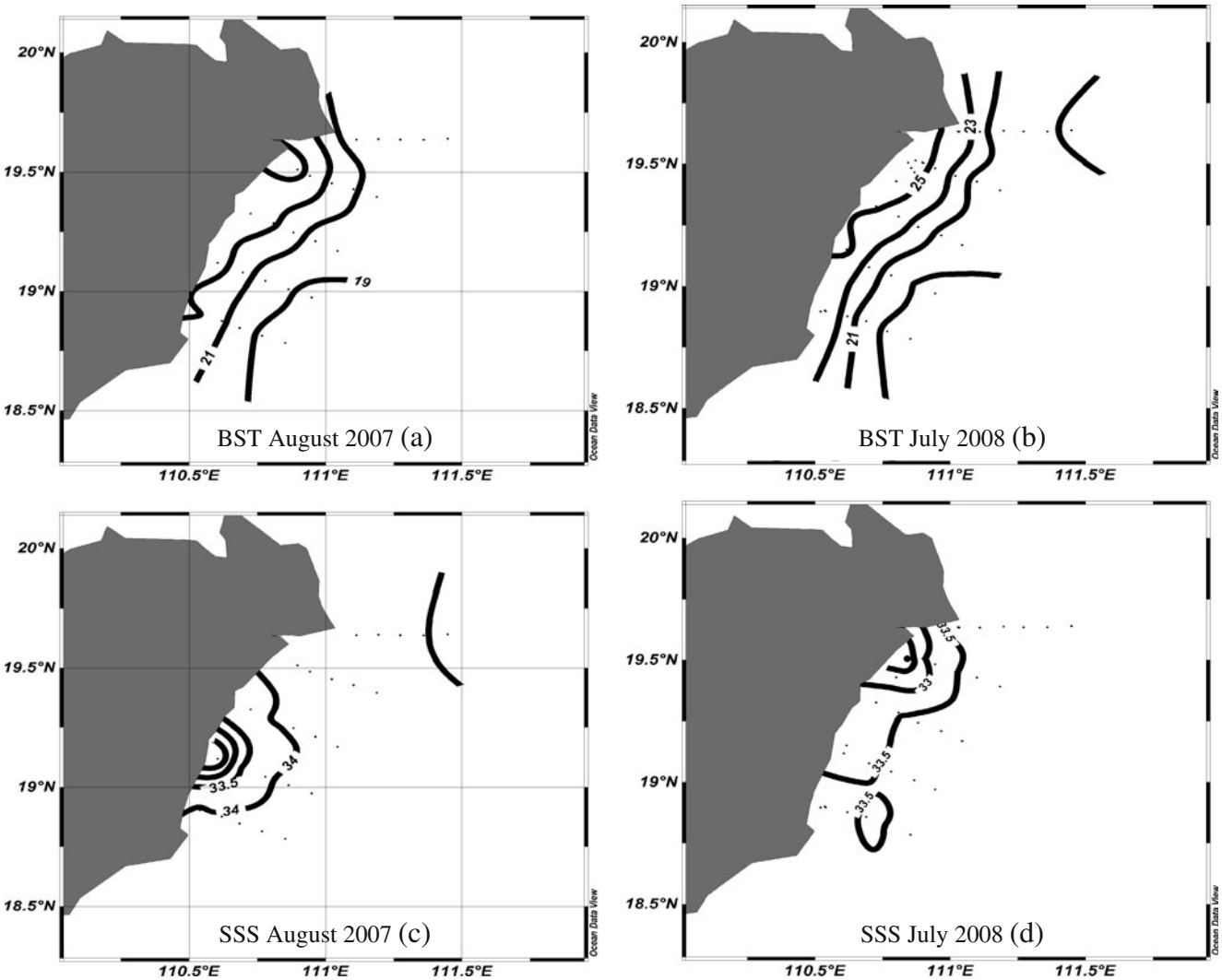

Fig. 4 Observed bottom temperature (*BST*) distribution (**a**, **b**) and surface salinity distribution (**c**, **d**) during the cruises August 2007 (**a**, **c**) and July 2008 (**b**, **d**). The Wanquan River plume is visible in 2007, whereas, Wenchang River plume has large influence on the shelf in 2008

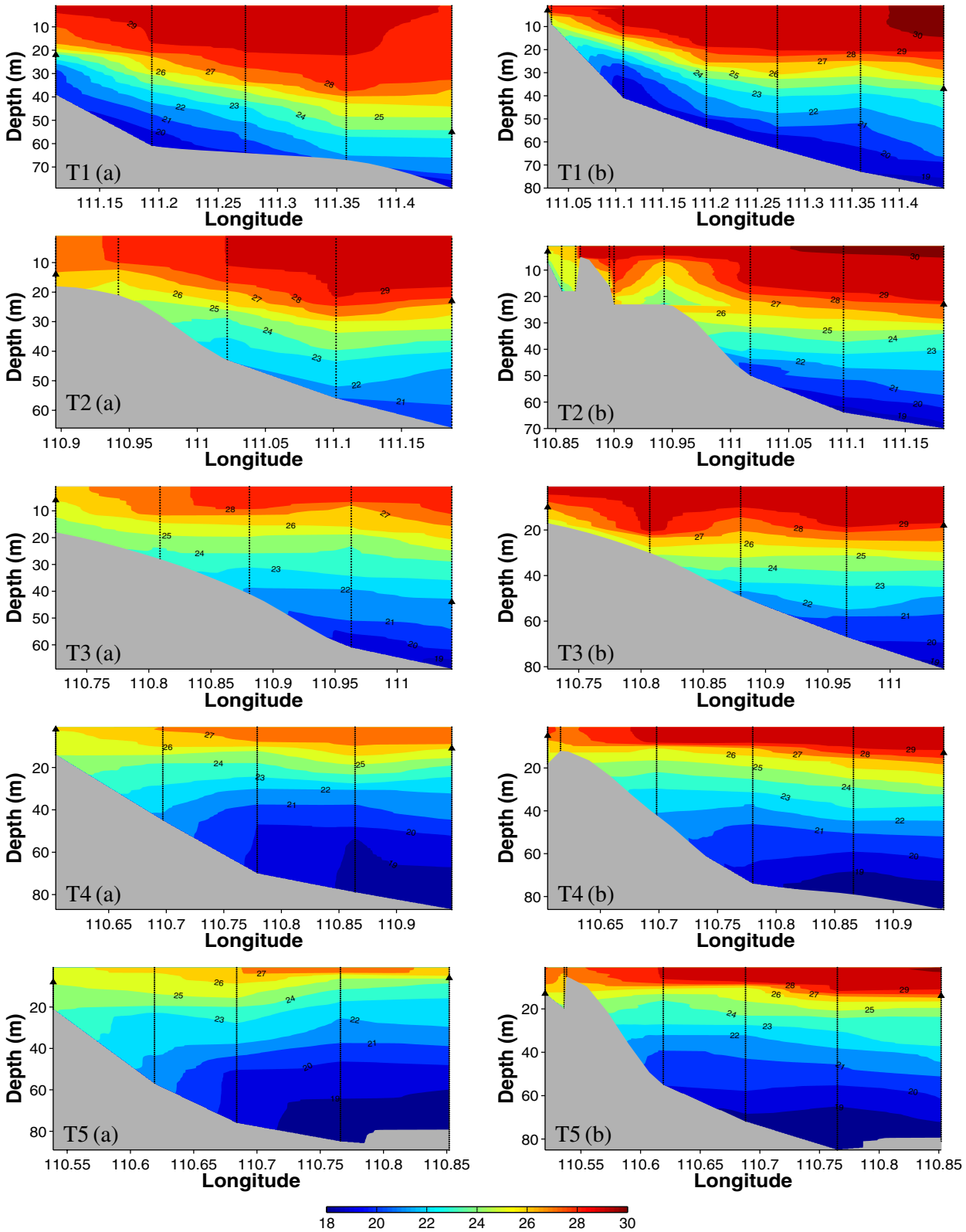

Fig. 5 Observed temperature (°C) distribution along sections T1–T5 during the cruise in August 2007 (**a**) and July 2008 (**b**). The *dotted lines* show the exact locations of the observation. We defined the vertical maximum temperature gradient as thermocline, and the locations of thermoclines at most nearshore and offshore stations were shown in the *figure with black triangle*. The thermocline uplift from the offshore station toward the nearshore station are 15, 21, 31, 8, and 1 m at T1–T5 in 2007 and 41, 20, 10, 25, and 2 m in 2008, respectively

a changed large scale advection field is responsible for the observed deviations.

Comparing the temperature distributions of all the sections in both years, the stratification in 2008 is stronger, and the mixed layer is thicker (Fig. 5). The average maximum vertical temperature gradient at the outer five stations in 2007 is 0.7°C/m and that in 2008 is 0.9°C/m. Obviously, there is an influence of strong turbulent mixing on the stability of the thermocline on the shelf. In particular, stratification was destroyed considerably at nearshore stations at section T5 (Fig. 5 T5(a)). Hence, a frontal structure was formed under the surface layer, separating the coastal mixed water from the stratified water (dashed line in Fig. 6).

A thermal front has been detected by satellite observations during summer off the northeastern Hainan coast (Hu et al. 2003). Fronts normally form natural barriers to the water transport (Wolanski and Hammer 1988) and, thus, decrease the horizontal and in turn vertical transport of the upwelled water masses. It has been shown that frontal zones could also be regions where the deep water is upwelled into the surface layer (Savidge 1976; James 1978; Lü et al. 2006). Nevertheless, the generation of the front under the post-storm stage off the northeastern Hainan coast is a temporary phenomenon, which is gradually developing, and thus does not support the prerequisite condition of a frontal induced upwelling.

In 2007, the temperature distribution at section T1 shows stratification at 20 m depth at the near coastal station and at 35 m depth at the offshore station, respectively, if we define the position of maximum vertical temperature gradient as the location of the thermocline (Fig. 5a). We noted the location of the thermocline in all sections in Fig. 5. Therefore, the thermocline was elevated by 15 m from the offshore station toward the nearshore station at section T1. We calculate thermocline uplift at all sections and the biggest difference of 25 m was found at section T1 between the two observations. In addition, the average uplift of the thermocline was 15 m in 2007 and 20 m in 2008. From this calculation, we could conclude that the uplift of the thermocline decreases under post-storm conditions.

From the observations, it is seen that the structure of the upwelling, i.e., the onshore site of the southern section T5 is the coldest, do not change from the pre-storm to the post-storm period. However, strong winds influence the stability of stratification and the uplift of cold water from deeper zones due to wind mixing causes an enhanced energy input. Consequently, the strength of the thermocline decreases by 0.2°C/m. This disturbance by the typhoon event is followed by a reequilibrium which also has an influence on water masses outside the shelf break, which in turn have an influence on the coastal environment.

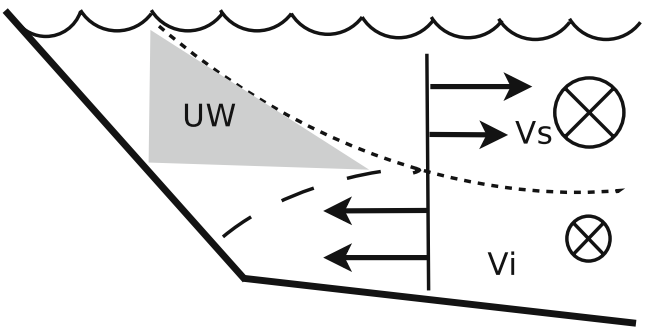

Fig. 6 Schematic of the circulation structure and isopycnals at a cross-shelf section on the eastern Hainan shelf. The *dotted line* represents isopycnal, while the *dashed line* shows the front structure when upwelling is not prevailing. The offshore velocity (*Vs*) in the surface boundary layer is a wind-driven flow. The onshore flow in the interior (*Vi*) balances the offshore transport. The bottom current is close to zero; hence, it is not shown in the figure. A geostrophic along-shelf current is in the direction of wind stress and decreases with depth. The *shaded area* represents the water masses which are lifted by upwelling (*UW*)

3.2 Cross-shelf momentum balance

A simple theory of wind-driven coastal upwelling related to the structure of the cross-shelf circulation was developed by Lentz and Chapman (2004). The theory predicts that the magnitude of the cross-shelf momentum flux divergence relative to the wind stress depends on the Burger number $S = \alpha\ N/f$, where α is the bottom slope, N is the buoyancy frequency, and f is the Coriolis parameter. For $S \ll 1$, the cross-shelf momentum flux divergence is small, the bottom stress balances the wind stress, and the onshore return flow occurs primarily in the bottom boundary layer. For $S \approx 1$ or larger (strong stratification), the cross-shelf momentum flux divergence balances the wind stress, the bottom stress is small, and the onshore return flow returns in the interior (Lentz and Chapman 2004).

We take section T2 as a typical section running from the estuary to the open ocean. Using the bottom slope (20 m depth difference by distance of 0.1°E), buoyancy frequency $\left(N = \sqrt{-\frac{g}{\rho_0}\frac{\partial \rho}{\partial z}} = \sqrt{\frac{9.8}{1021}\frac{3}{50}} = 0.024\,\mathrm{s}^{-1}\right)$, and Coriolis parameter based on the observations in 2008 along this section (Table 1), it is possible to calculate a Burger number S of 0.91. In other sections, S values are also close to 1. Comparing these parameters with other typical wind-driven upwelling systems in the world, it

Table 1 Parameters at section T2 (Fig. 1) on Eastern Hainan shelf derived from observations: α is the bottom slope, N is the buoyancy frequency, f is the Coriolis frequency, and $S = \alpha\ N/f$ is the Burger number

	α (10^{-3})	N (10^{-3} s^{-1})	f (10^{-4} s^{-1})	S
Hainan	1.8	24	0.47	0.91
Peru	10	5.5	−0.38	1.5
Oregon	6.7	14.6	1.03	0.95
Northern California	5	6.8	0.91	0.38

We compare the estimation with that of sites off Peru, Oregon, and northern California, which were estimated by Lentz and Chapman (2004)

shows that stratification is the strongest among them and the bottom slope is relatively small. Based on this theory, the wind stress is balanced by the cross-shelf momentum flux and the onshore return flow occurs in the inner-part of the water column. Based on the current measurements along section T2 (Fig. 7c), we obtained the cross-shelf and along-shelf components of the mean currents (Fig. 7a, b). The mean current at 15 m showed an onshore component. These results also support the conclusion from theory that the return flow takes place in the interior and not in the bottom layer. It is worth noting that we did not obtain an offshore current component at a depth of 5 m. We believe that this is due to the specific shape of the coastline in this area. The section T2 is located at the upstream side of a cape, where topographic influence drives the current toward the coast due to the conservation of potential vorticity. The current pattern in the modeling study of Su and Pohlmann (2009) also suggested that the surface current along T2 is onshore.

Based on the theory of Lentz and Chapman (2004), we can draw a schematic of the circulation pattern along a cross-shelf section off the eastern Hainan coast (Fig. 6). In a study of a comparable weak upwelling system, i.e., upwelling off Oregon, Huyer (1983) found that the offshore Ekman transport is carried by the surface Ekman layer, and the onshore return flow occurs through the quasi-geostrophic interior. Our studies lead

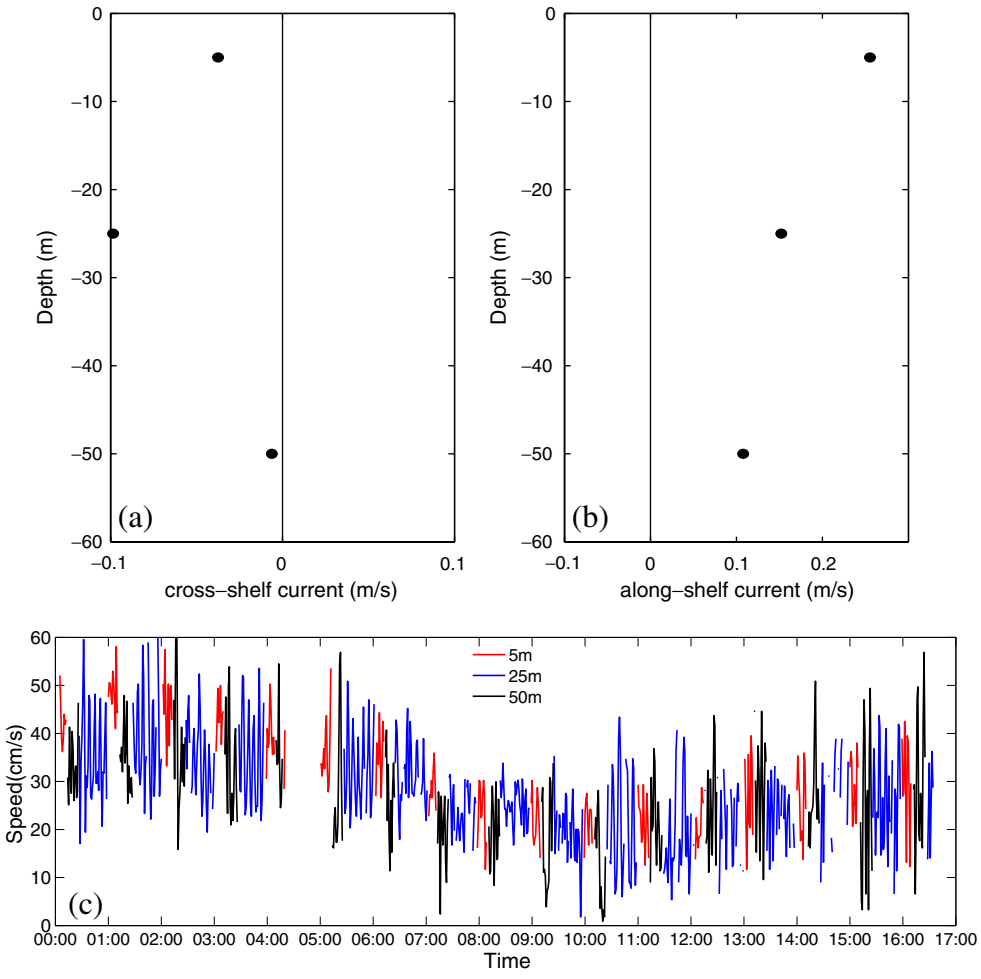

Fig. 7 Cross shelf (**a**) and along shelf (**b**) mean current profiles at the anchor station (Fig. 1). Positive currents are offshore and poleward, respectively. The angle between the coastline and meridian is 60°. The measured current speeds at 5, 25, and 50 m (**c**), respectively, show that a flood and ebb event was captured

to the conclusion that the onshore transport required to balance the wind-driven offshore transport occurs mainly in the interior. Using this analysis, we can estimate the upwelling water fluxes even if we have only a basic understanding of the structure of the cross-shelf circulation, and it is not necessary to have a detailed knowledge of the flow in the bottom boundary layer.

4 Discussion

4.1 The response of the estuaries to the typhoon and precipitation events and how estuaries affect upwelling

Since there exist two estuaries in Wenchang Bay, it is important to study the variability of estuarine water masses, in particular its sensitivity to upwelling. The salinity distribution along the topography following sections shows that the freshwater can only reach offshore to the 20-m isobath, which is the outer limitation of influenced area by river plume. In order to clarify the impact of freshwater on upwelling, we calculated the potential energy anomaly ϕ in the observation area in 2008 (Fig. 8). The potential energy (PE) anomaly has been defined by Simpson and Bowers (1981) and developed by Burchard and Hofmeister (2008) as the amount of mechanical energy required to homogenize the water column. $\phi = -\frac{1}{H}\int_{-H}^{0} gz(\overline{\rho} - \rho)dz$, where ρ is the density at a certain depth, $\overline{\rho}$ is the depth-mean density, H is water depth, and g is gravitational acceleration. The calculation of ϕ was aimed at understanding the gradient of PE from onshore to offshore and relative PE change in the inner shelf, which was not for quantitative estimation. In general, PE is related to the stratification, while upwelling is accompanied by low PE, i. e., a reduced stratification. In contrast, buoyancy forcing from the river enlarges PE and increases stratification. Therefore, ϕ is higher when the water column is more stable, while $\phi = 0$ indicates a well-mixed water column. In the offshore part of the observed area (depth >50 m), the isoline of PE runs parallel to the isobath, indicating the influence of topography. In contrast, the mismatch of PE with bathymetry isolines in the nearshore area (depth >50 m) demonstrates an influence of other destabilizing factors, e.g., a strong mixing. Looking at the PE in the Wenchang estuary, it is clear that PE increased at the mouth of the river outflow. The explanation for this is that the freshwater discharge stabilizes the water column, thereby inhibiting the upwelling. Of course, this process is only confined to the near coastal area, which does not have a significant impact on the upwelling strength on the shelf itself. This phenomenon can also be found in other regions where the interaction between upwelling and river discharge takes place, e.g., the upwelling in California current system and the Columbia River (Hickey et al. 2005; Hickey and Banas 2008).

In Section 3.1, it was mentioned that the low salinity of the Wanquan River estuary in 2007 was related to the typhoon event (Fig. 4c). On the contrary, in 2008, Wenchang River had a big influence on the Wenchang Bay, and the influence of the Wanquan River is not apparent in the adjacent coastal waters in that year (Fig. 4d). We first look at the differences of these two river systems.

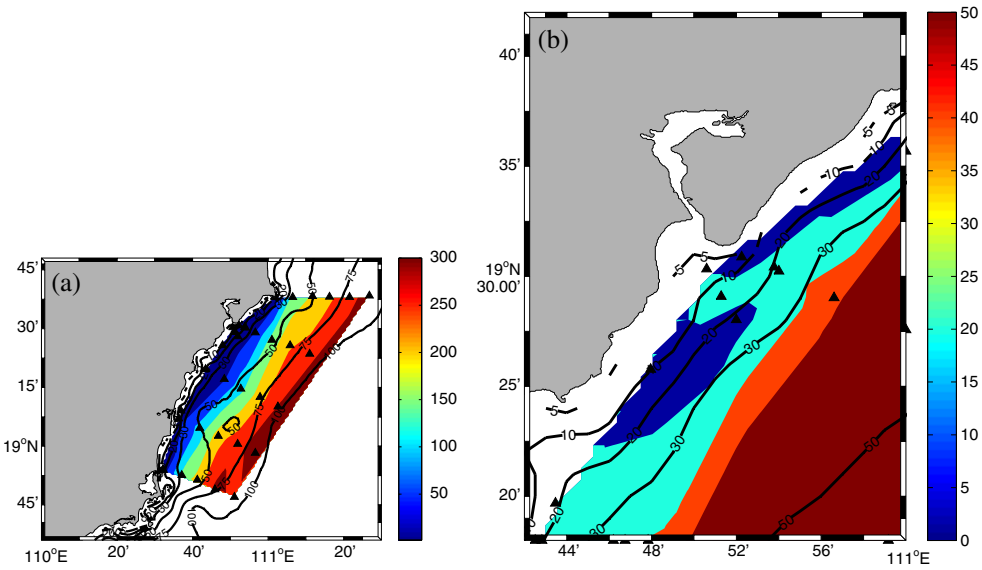

Fig. 8 The *color-shaded plots* show observed potential energy (PE) distribution in July 2008. The *background contour lines* represent bathymetry. The low PE near the coast indicate the strong mixing area (**a**). When having a detail view of the estuarine area, the increase of PE indicates the increase of the stability. Hence, the estuarine water locally inhibits the upwelling (**b**)

The Wanquan River annual mean discharge is 164 m^3/s (Ge et al. 2003), and the Wenchang River is composed of several small rivers, including a small bay, i.e., Bamen Bay (Fig. 1), but the total discharge is less than the Wanquan. The Wanquan River mouth is narrow due to a dike construction. Therefore, we could speculate that the residence time in the Wenchang River is higher, which is not only due to its shape but also because of the lower salinity in the Wenchang Bay. From the precipitation data in Haikou and Qionghai (Fig. 9), we could infer the river discharge differences in both years. The typhoon brought strong precipitation which after 1 week had only significantly affected the Wanquan River estuary, although the precipitation in Haikou seems higher than that in Qionghai in August 2007. This confirms that the Bamen Bay in the Wenchang River system increases the residence time of the freshwater discharge leading to a much slower influence from the typhoon. In contrast, the salinity gradient off the Wanquan River is stronger in the post-storm stage, indicating that freshwater is directly transported to the estuary and coastal waters, leading to a faster response. Therefore, the fact that less precipitation in Qionghai leads to lower salinity in the Wanquan River compared to the Bamen Bay could only be attributed to the specific shape of the both river mouth systems. In

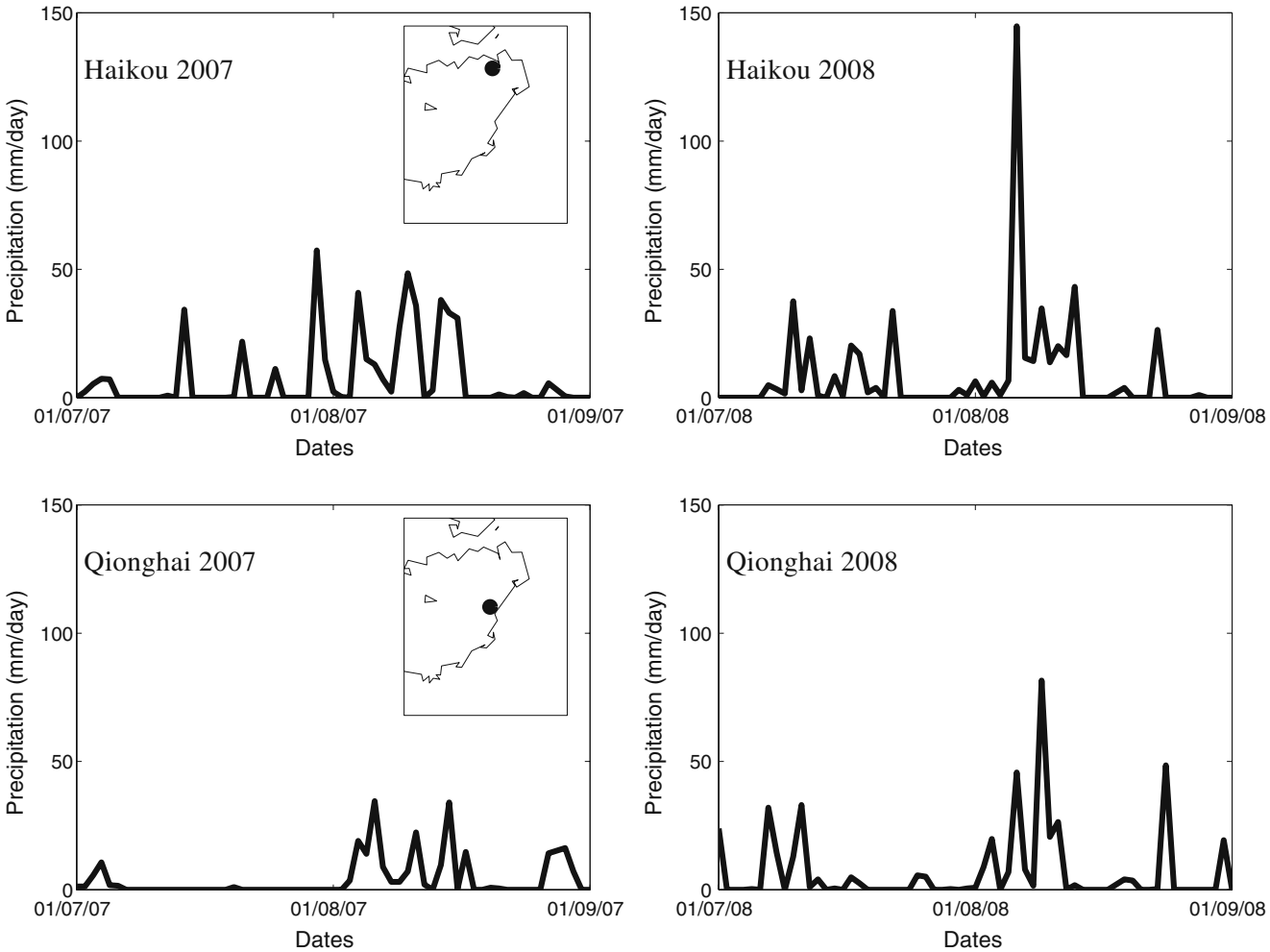

Fig. 9 The precipitation data (millimeters per day) in Haikou and Qionghai stations in July and August in 2007 and 2008. The location of two stations are showed with *black dots*. The Haikou station is close to Wenchang River, and the Qionghai station is close to Wanquan River. The precipitation data could give a certain estimation of two river discharges, respectively. The typhoon in 2007 brought more precipitation in Haikou, while there was strong precipitation 1 week before the observation in Qionghai. The precipitation in Haikou in July 2008 lasted longer than that in Qionghai

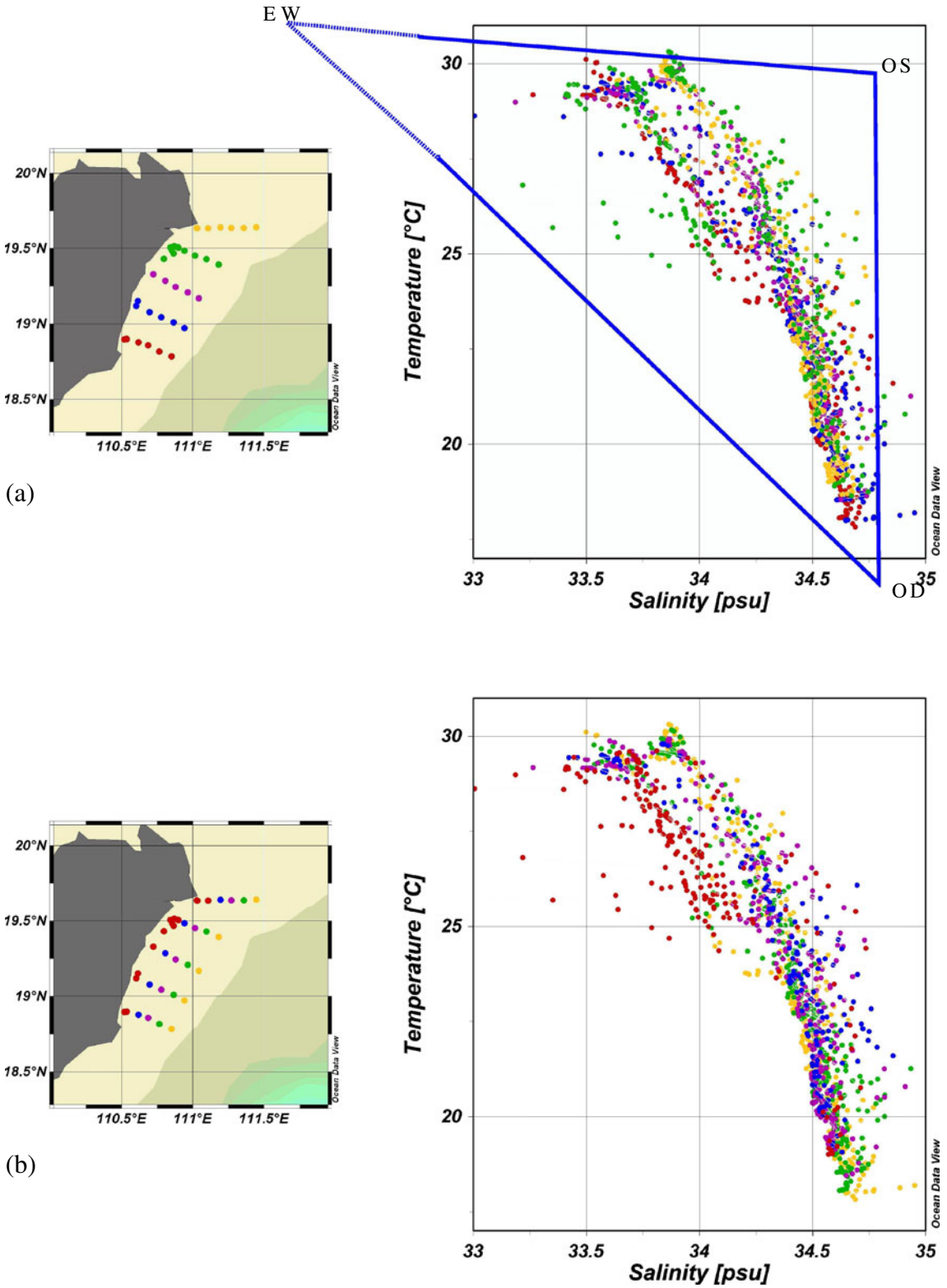

Fig. 10 *T*, *S* diagrams during the cruises in July 2008. *Different colors* indicate different sections in **a**. The *blue lines* form a *triangle*, bordered by three water masses, i.e., estuarine water (*EW*), offshore surface water (*OS*), and offshore deep water (*OD*), respectively. *Different colors* indicate different water depth at the stations in **b**. Most near coast stations in all sections forms a separate water mass in the *T*–*S* diagram

contrast, in July 2008, the precipitation in Haikou lasted longer so that the flow from the Wenchang River to the estuary was slower but more steady, and the Wanquan River water is quickly diluted in the bay. This is the reason for a weaker salinity gradient off the Wenchang River estuary in 2008, compared to the situation off the Wanquan River in 2007. However, we need more data to fully explain the investigated results.

We attempt to clarify how the estuary and the upwelling water interact in this region by means of a water mass analysis. In particular, this analysis will focus to put on the fact how the estuary affects the upwelling strength. The different water masses on the eastern Hainan shelf are generally showing the mixing of two water masses. Normally, we would expect T–S values to be located within a triangle, bordered by three water masses, i.e., freshwater from river load, offshore surface water, and offshore deep water, respectively (Fig. 10a). Since the part of the water mass with the influence of freshwater is missing, we may speculate that the influence of rivers on the shelf is limited. Interestingly, the near coastal stations show a different slope in the T–S diagram (Fig. 10b), from which we can conclude that the water masses are separated into mixed and estuarine waters. The freshwaters are confined to the coastal area less than 20–30 m deep.

4.2 Estimation the vertical transport

Finally, we aim at a qualitative estimation of the water mass transported into the coastal area by an upwelling event. There are several methods to estimate the upwelling strength. A common way to obtain a rough estimate of the amount of upwelled water and nutrients transported into the surface layer by upwelling is to multiply the average increase of nutrient concentration by the volume of the affected water mass (Lips et al. 2009). To consider a quasi-equilibrium upwelling state for this estimation, we choose a stronger upwelling event (i.e., the upwelling in July 2008), since the upwelling favorable southerly wind dominated the entire month before the observation. The upwelling is controlled by intermittent wind direction variation, and the development of the upwelling in this region takes about 1 month, as Su and Pohlmann (2009) concluded from model studies. The given value for upwelling fluxes thus provides a good estimation for an upwelling event. The QuikSCAT wind stress in July 2008 along the eastern Hainan coast is used to calculate the Ekman transport (ME). ME along the T2 section is about 2,000 $\mathrm{kg\,m^{-1}\,s^{-1}}$. The width of the upwelling region (B) is about 60 km (comparable to the horizontal scale used in the next paragraph). The vertical compensation water velocity (w) is $w = \mathrm{ME}/\rho \cdot B$, where ρ is water density. Therefore, the resulting vertical velocity according to classic Ekman theory is about 2.8 m/day. The upwelling at eastern Hainan is associated with a strong stratification, which leads to the consequence that the transport rates estimated by the classic Ekman theory accounting only for the barotropic conditions may lead to an overestimation. Due to a positive stability of the water column, additional energy is needed to uplift the respective water mass. For this reason, it is not possible to define a simple balance as for the Benguela upwelling system and the upwelling

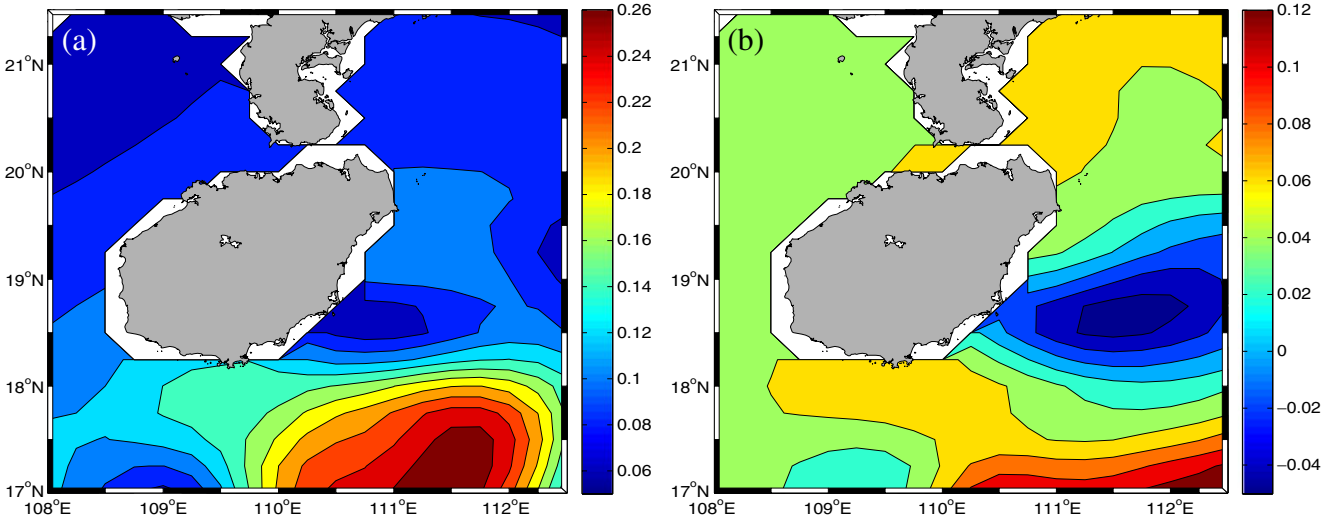

Fig. 11 MODAS SSH on 20 August 2007 (**a**) and on 28 July 2008 (**b**). Large-scale eddy can be observed close to the bay where the detailed estuarine observations took place in both years

system Off Oregon, where Ekman suction induced by wind stress curl was the major contributor to the total upward velocity (Halpern 1976; Fennel 1999).

Here, we use a schematic plot to describe our conceptual model to roughly estimate the vertical water fluxes (Fig. 6). Upwelling develops when interior water breaks a front and thermocline reaches the coastal area. Therefore, upwelled water volume could be roughly estimated by vertical distance of the thermocline raising from the offshore to the coast (shaded area in Fig. 6). Of course, the error of this estimation might be relatively large, since the strength and duration of the wind cannot be fully accounted for. Taking section T2 as a reference section, the thickness of the upper mixed layer near the shelf break station is about 35 m, whereas in the estuary it is about 15 m. The distance from the station furthest offshore to the estuary is about 60 km. Thus, the uplifted water along one section of unit width amounts to 600,000 m^2. The coastline of the observation area is about 100 km long. Therefore, the total amount of uplifted water by upwelling is equal to approximately 60 km^3. The development of the upwelling in this region takes about 1 month Su and Pohlmann (2009). Therefore, a simple calculation of the uplift rate of the thermocline is 0.67 m/day (20 m/30 day), the magnitude is comparable to the calculation of Ekman suction off Peru (Halpern 2002). The upwelling flux is about 2 km^3/day, which is a minimum value of a strong upwelling in this region. From this, we can estimate the total nutrient transport by knowing the nutrient concentrations of the sub-thermocline water mass off the shelf break.

Of course, a large uncertainty could be expected in the estimation of the vertical transport, e.g., we only took the section T2 into account. At sections T3–T5, the thermocline is relatively flat comparing to T1 and T2. From SSH pictures, we found that cyclonic eddies occur at a latitude of 18.5° N in both observational periods (Fig. 11). SST pictures consistently show cold water centers at the same latitude (Fig. 3). When a cyclonic eddy approaches the coast, the thermocline will descend from the ocean toward the land. Normally, non-local impacts cannot be considered when studying coastal upwelling events. Nevertheless, the influence of mesoscale eddies should not be ignored. The size of cold eddies approaching to the Wenchang Bay is larger than 100 km as can be inferred from satellite pictures. The amount of intruded cold water is relatively equal to the water volume on the inner shelf, which means that eddies will bring a significant amount of instability to the upwelling system. This uncertainty estimation can only be resolved with the approach of integrating data into numerical modeling.

5 Conclusions

The response of the eastern Hainan shelf to upwelling events is studied by means of cruise data combined with SST and SSH data from 2007 and 2008. Based on hydrodynamical observations, we found that the distribution of upwelling centers along eastern Hainan Island is relatively stable, whereas strong winds lead to high instabilities of stratification on the shelf. Some conclusions can be drawn from a basic analysis: (1) We calculate the Burger number to be $S \approx 1$, indicating that the cross-shelf momentum flux divergence balances the wind stress and the onshore return flow occurs in the interior of the water column, which agrees nicely with our results of current measurements. (2) The strong mixing caused by typhoons reduces the strength of the thermocline, particularly in the coastal area. The front between the mixed coastal water and offshore water is established, which in turn weakens upwelling strength. (3) The freshwaters from the two main rivers in the Wenchang Bay are confined to the coastal area inside the 20–30 m isobath, as confirmed by water mass analysis. Therefore, estuarine waters do not have a significant impact on the upwelling.

Acknowledgements We thank Dr. Daoru Wang for the preparation for the cruises, Dr. Daniela Unger for the information of precipitation data, Dr. Xiaopei Lin for the valuable discussion, and Kieran O'Driscoll for revising the paper. This work was performed in the frame of the project "Land-Sea Interactions along Coastal Ecosystems of Tropical China: Hainan (LANCET)" under grant number BMBF-03F0457B and BMBF-03F0620B. We are grateful to two anonymous reviewers for their constructive comments, which improved the manuscript.

References

Allen JS (1973) Upwelling and coastal jets in a continuously stratified ocean. J Phys Oceanogr 3(3):245–257

Allen JS, Newberger PA, Federiuk J (1995) Upwelling circulation on the Oregon continental shelf. Part I: response to idealized forcing. J Phys Oceanogr 25(8):1843–1866

Burchard H, Hofmeister R (2008) A dynamic equation for the potential energy anomaly for analysing mixing and stratification in estuaries and coastal seas. Estuarine Coastal Shelf Sci 77(4):679–687

Federiuk J, Allen JS (1995) Upwelling circulation on the Oregon continental shelf. Part II: simulations and comparisons with observations. J Phys Oceanogr 25(8):1867–1889

Fennel W (1999) Theory of the Benguela upwelling system. J Phys Oceanogr 29(2):177–190

Gan J, Allen JS (2002) A modeling study of shelf circulation off northern California in the region of the Coastal Ocean Dynamics Experiment: response to relaxation of upwelling winds. J Geophys Res 107:3123

Ge C, Slaymaker O, Pedersen T (2003) Change in the sedimentary environment of Wanquan River Estuary, Hainan Island, China. Chin Sci Bull 48(21):2357–2361

Guo F, Shi MC, Xia ZW (1998) Two-dimensional diagnose model to calculate upwelling on offshore of the east coast of Hainan Island (in Chinese). Acta Oceanol Sin 20(6):109–116

Halpern D (1976) Measurements of near-surface wind stress over an upwelling region near the Oregon coast. J Phys Oceanogr 6(1):108–112

Halpern D (2002) Offshore Ekman transport and Ekman pumping off Peru during the 1997–1998 El Nino. Geophys Res Lett 29(5):1075

Hickey B, Geier S, Kachel N, MacFadyen A (2005) A bi-directional river plume: the Columbia in summer. Cont Shelf Res 25(14):1631–1656

Hickey BM, Banas NS (2008) Why is the northern end of the California current system so productive? Oceanogr 21(4):90–107

Hu JY, Kawamura H, Tang DL (2003) Tidal front around the Hainan Island, northwest of the South China Sea. J Geophys Res O 108(C12):3342. doi:10.1029/2003JC001883,3379

Huyer A (1983) Coastal upwelling in the California Current system. Prog Oceanogr 12(3):259–284

James ID (1978) A note on the circulation induced by a shallow-sea front. Estuar Coast Mar Sci 7(2):197–202

Jing Z, Qi Y, Hua Z, Zhang H (2009) Numerical study on the summer upwelling system in the northern continental shelf of the South China Sea. Cont Shelf Res 29(2):467–478

Kara AB, Barron CN (2007) Fine-resolution satellite-based daily sea surface temperatures over the global ocean. J Geophys Res 112:C05041. doi:10.1029/2006JC004021

Lentz SJ (1992) The surface boundary layer in coastal upwelling regions. J Phys Oceanogr 22(12):1517–1539

Lentz SJ, Chapman DC (2004) The importance of nonlinear cross-shelf momentum flux during wind-driven coastal upwelling. J Phys Oceanogr 34(11):2444–2457

Lips I, Lips U, Liblik T (2009) Consequences of coastal upwelling events on physical and chemical patterns in the central Gulf of Finland (Baltic Sea). Cont Shelf Res 29(15):1836–1847. doi:10.1016/j.csr.2009.06.010

Lü X, Qiao F, Xia C, Zhu J, Yuan Y (2006) Upwelling off Yangtze River estuary in summer. J Geophys Res O 111(C11):C11S08

Lü X, Qiao F, Wang G, Xia C, Yuan Y (2008) Upwelling off the west coast of Hainan Island in summer: its detection and mechanisms. Geophys Res Lett 35(2):L02,604

Monteiro P, Largier J (1999) Thermal stratification in Saldanha Bay (South Africa) and subtidal, density-driven exchange with the coastal waters of the Benguela upwelling system. Estuar Coast Shelf Sci 49(6):877–890

Ning X, Chai F, Xue H, Cai Y, Liu C, Shi J (2004) Physical–biological oceanographic coupling influencing phytoplankton and primary production in the South China Sea. J Geophys Res O 109(C10):c10005

O'Brien JJ, Hurlburt HE (1972) A numerical model of coastal upwelling. J Phys Oceanogr 2(1):14–26

Pedlosky J (1978) An inertial model of steady coastal upwelling. J Phys Oceanogr 8(2):171–177

Savidge G (1976) A preliminary study of the distribution of chlorophyll a in the vicinity of fronts in the Celtic and western Irish Seas. Estuar Coast Mar Sci 4(6):617–625

Simpson JH, Bowers D (1981) Models of stratification and frontal movement in shelf seas. Deep Sea Res I 28(7):727–738

Smith RL (1995) The physical processes of coastal ocean upwelling systems. In: et al CPS (ed) Upwelling in the ocean: modern processes and ancient records. Wiley, New York, pp 39–64

Su J, Pohlmann T (2009) Wind and topography influence on an upwelling system at the eastern Hainan coast. J Geophys Res 114(C6):C06,017

Su JL (2004) Overview of the South China Sea circulation and its influence on the coastal physical oceanography outside the Pearl River Estuary. Cont Shelf Res 24(16):1745–1760. doi:10.1016/j.csr.2004.06.005

Wolanski E, Hammer WM (1988) Topographically controlled fronts in the ocean and their biological influence. Science 241(4862):177–181

Ye L (1988) A typical estuary consisting of a tidal inlet and lagoon system and its engineering significance. Estuaries and Coasts 11(4):250–254